

NATIONAL ADVISORY COMMITTEE FOR AERONAUTICS

# WARTIME REPORT

ORIGINALLY ISSUED

May 1945 as  
Memorandum Report A5E03

THE EFFECT OF MACH NUMBER ON THE AERODYNAMIC  
CHARACTERISTICS OF A SINGLE-ENGINE PURSUIT  
AIRPLANE AS DETERMINED FROM TESTS OF A  
1/3-SCALE MODEL

By Robert C. Robinson and Henry Jessen

Ames Aeronautical Laboratory  
Moffett Field, California

# NACA

WASHINGTON

NACA LIBRARY  
LANGLEY AERONAUTICAL LABORATORY  
Hampton, Virginia

NACA WARTIME REPORTS are reprints of papers originally issued to provide rapid distribution of advance research results to an authorized group requiring them for the war effort. They were previously held under a security status but are now unclassified. Some of these reports were not technically edited. All have been reproduced without change in order to expedite general distribution.



MR.No. A5303

NATIONAL ADVISORY COMMITTEE FOR AERONAUTICS

MEMORANDUM REPORT

for the

Air Technical Service Command, U. S. Army Air Forces

THE EFFECT OF MACH NUMBER ON THE AERODYNAMIC  
CHARACTERISTICS OF A SINGLE-ENGINE PURSUIT AIRPLANE  
AS DETERMINED FROM TESTS OF A  
1/3-SCALE MODEL

By Robert C. Robinson and Henry Jessen

SUMMARY

Presented herein are the results of tests to determine the effects of Mach number on the aerodynamic characteristics of an Allison powered single-engine pursuit airplane. The lift, drag, and pitching-moment characteristics at high speed are discussed and data are included to show the variation of stability, tail effectiveness, and elevator effectiveness with Mach number. The increments of drag and pitching moment due to a deflector vane in front of the radiator scoop are presented.

INTRODUCTION

Although a model of a Merlin powered version of the airplane had been tested previously in the Ames 16-foot wind tunnel (reference 1), it was desired to obtain data on a model of the Allison version of the airplane for correlation with the results of flight tests under way at the Langley Memorial Aeronautical Laboratory. The investigation was carried out at the request of the Air Technical Service Command, U. S. Army Air Forces.

Both pressure-distribution measurements and force tests were included. This report deals with the aerodynamic characteristics in pitch as obtained from the force tests.

Data are included to show the effects of Mach number on the stability and on the elevator and horizontal-tail effectiveness.

On some early versions of the airplane, a retractable deflector vane was used in front of the radiator scoop to prevent overcooling during dives. Pilots have reported that, in dives with this vane extended, longitudinal oscillations of the airplane develop at a higher Mach number than with the vane retracted. Tests were made at lift coefficients ranging from  $-0.04$  to  $0.4$  with the vane attached to the model in order to investigate its effects on drag and pitching-moment coefficients.

Dive-recovery flaps were present on the airplane making the flight tests. In order that the model would more closely represent the airplane, tests were made with a simulation of these flaps, in the retracted position, attached to the model.

Most of the figures presented are cross plots from the data plotted against Mach number and elevator angle, and consequently the experimental points are not shown.

## APPARATUS

The  $1/3$ -scale model was designed and built at the Ames Aeronautical Laboratory and is similar in construction to the model described in reference 1. The two models represented airplanes which differed mainly in the lines of the forward part of the fuselage and the vertical location of the wing. Changing from the Allison engine to the Merlin engine (reference 1) made it necessary to change the forward lines of the fuselage, the carburetor air scoop being moved from the top to the bottom of the nose. Also, for the Merlin version of the airplane the wing was lowered 1 inch (model dimension) and the size and lines of the cooling-air duct were changed. The horizontal tail on the model in this report was the same as the standard tail of reference 1. Sealed gun openings in the wings, dummy gun cowlings on the forward part of the fuselage, and an optograph cover on the top of the aft portion of the

fuselage were added to the basic model. The exit flaps of the cooling-air ducts were in the flush position for all tests. A three-view drawing of the model is shown in figure 1, and the wind-tunnel setup is illustrated in the photograph of figure 2. Figure 3 shows the radiator deflector vane in place on the model.

The model was mounted in the tunnel on a three-strut support system with two 5-percent-thick front struts and a 7-percent-thick rear strut. The front struts were spaced 80 inches apart and the trunnion was 25 percent of the chord aft of the leading edge.

The following is a list of pertinent dimensions of the model:

Wing area, sq ft . . . . .	25.91
Span, ft . . . . .	12.34
Mean aerodynamic chord, ft . . . . .	2.21
Aspect ratio of wing . . . . .	5.89
Tail length (25 percent M.A.C. to elevator hinge line), ft . . . . .	5.75
Horizontal-tail area, sq ft. . . . .	4.66
Horizontal-tail span, ft . . . . .	4.39
Aspect ratio of horizontal tail plane . . . . .	4.14
Normal stabilizer incidence relative to fuselage reference line, deg . . . . .	2
Elevator area aft of hinge line (each), sq ft. . . . .	0.723
Mass-balance paddle area (each), sq ft . . . . .	0.028
Elevator-tab area (each), sq ft. . . . .	0.106
Elevator span at hinge line (each), ft . . . . .	2.043

## Normal center-of-gravity location

Percent mean aerodynamic chord . . . . . 26.0

Distance below fuselage reference line, in . . . . . 3.18

## SYMBOLS

The symbols used in this report are defined as follows:

V	free-stream velocity, feet per second
$\rho$	mass density of air, slugs per cubic foot
q	free-stream dynamic pressure ( $\frac{1}{2}\rho V^2$ ), pounds per square foot
M	Mach number $\left( \frac{V}{\text{velocity of sound}} \right)$
S	wing area, square feet
M.A.C.	mean aerodynamic chord, feet
$C_L$	lift coefficient $\left( \frac{\text{lift}}{qS} \right)$
$C_D$	drag coefficient $\left( \frac{\text{drag}}{qS} \right)$
$C_{m.c.g.}$	pitching-moment coefficient about the center of gravity $\left( \frac{\text{pitching moment about the center of gravity}}{q S M.A.C.} \right)$
$\alpha$	angle of attack of fuselage reference line corrected for tunnel-wall effects and upflow due to support struts, degrees
$\alpha_u$	uncorrected angle of attack of fuselage reference line, degrees
$i_t$	incidence of horizontal stabilizer with respect to the fuselage reference line, degrees
$\Delta C_m$	increment of pitching-moment coefficient
$\Delta C_D$	increment of drag coefficient

## WIND-TUNNEL CALIBRATION AND CORRECTIONS

The dynamic pressures and Mach numbers were determined by means of a static-pressure survey in the region of the tunnel occupied by the model. All three struts were in place during the survey. The results obtained were corrected for the constriction effect of the model. A detailed description of the survey method and the constriction correction are given in reference 2.

Tunnel-wall, tare, and upflow corrections were applied to all the data. The tunnel-wall corrections were calculated by the method of reference 3. Drag and pitching-moment tares due to the support struts were evaluated from force tests of the struts alone. In order to find the upflow effects caused by the front struts, tests were made with the model erect and inverted. One-half the difference between the angles of zero lift for the two conditions was taken as the upflow angle. The following table lists the corrections that have been applied:

H	$\Delta C_{D_{upflow}}$	$\Delta \alpha_{upflow}$ (deg)
0.4 - 0.690	0.00175 $C_L$	0.10
.7	.00320 $C_L$	.18
.725	.00545 $C_L$	.31
.75	.00735 $C_L$	.42
.775	.00925 $C_L$	.53
.8	.01135 $C_L$	.64
.81	.01205 $C_L$	.69

$$\Delta\alpha = \frac{1}{8} \cdot \frac{25.91}{201.6} 573 C_L = .1923 C_L$$

Angle-of-attack correction =  $1.019 C_L + \Delta\alpha_{\text{upflow}}$

Drag-coefficient correction =  $0.0178 C_L^2 + \Delta C_{D_{\text{upflow}}} + \Delta C_{D_{\text{tare}}}$   
 $= 0.0178 C_L^2 + \Delta C_{D_{\text{upflow}}} - 0.010$

Pitching-moment-coefficient

correction =  $0.0118 C_L + \Delta C_{m_{\text{tare}}}$   
 $= 0.0118 C_L + 0.0220$

## RESULTS AND DISCUSSION

### Longitudinal Characteristics

The lift coefficient for the model without and with the tail surfaces (figs. 4 and 5, respectively) has been plotted in carpet form to show simultaneously its variation with Mach number and angle of attack. The pitching-moment coefficient is also plotted in carpet form (fig. 6) to show its variation with lift coefficient for various Mach numbers. Figure 6 shows that the static longitudinal stability  $-\partial C_m / \partial C_L$  at the lift coefficient for balance with the elevators neutral changed from 0.078 at a Mach number of 0.4 to 0.203 at a Mach number of 0.8 - an increase of 160 percent. For the same range of Mach numbers the lift coefficient for balance decreased from 0.065 to -0.125.

The variation of drag coefficient with lift coefficient is shown in figure 7 for several Mach numbers, and the effect of Mach number on the drag and pitching-moment coefficients for various lift coefficients is shown in figure 8.

The above Mach number effects are similar to those found for the model of the Merlin powered version of the airplane, and their influence on the longitudinal-control characteristics is discussed in reference 1.

### Elevator and Tail Effectiveness

The effect of elevator deflection upon the pitching-moment coefficient is presented in figures 9(a) to 9(g). For the same elevator deflections ( $-5^\circ$  to  $3^\circ$ ) the change of

lift coefficient was roughly 0.006 per degree. The maximum change of drag coefficient due to the  $11^\circ$  change of elevator deflection varied from 0.002 to 0.015, depending on the angle of attack and Mach number. From figure 10 it can be seen that the decrease of elevator effectiveness with Mach number was small enough to be unimportant.

The increment of pitching-moment coefficient resulting from changes in stabilizer incidence and the effect of Mach number on tail effectiveness are shown in figures 11 and 12. For negative stabilizer angles and the higher Mach numbers, the tail effectiveness decreased for large negative angles of attack. This decrease was evidently due to shock stalling of the horizontal tail caused by the large angle of attack and high Mach number.

With the standard stabilizer incidence and for small angles of attack, the tail effectiveness increased slightly with Mach number up to 0.765. At 0.4 Mach number the tail effectiveness was about 1.5 times as great as that for the elevator, and at 0.765 it was about 2.1 times as great. The fact that the elevator has less effect on the pressure distribution over the stabilizer at high Mach numbers and the increase of lift-curve slope with Mach number for the horizontal tail with elevator neutral account for this change. It appears that, as higher Mach numbers are reached, a controllable stabilizer or an all-movable tail plane will become more desirable from purely aerodynamic considerations.

## Effects of Deflector Vane and Retracted

### Dive-Recovery Flaps

Extension of the deflector vane in front of the cooling-air scoop caused a positive increment in pitching-moment coefficient of about 0.008 which was practically unaffected by Mach number or small changes of angle of attack. The drag increment was negligible up to a Mach number of about 0.75, but at 0.8 it varied from 0.004 to -0.006, depending on the angle of attack. However, the variation with angle of attack was rather inconsistent, as shown in figure 13. Neither the drag nor pitching-moment-coefficient increments offer an explanation for the effect the deflector vane was reported to have on the airplane in dives.



The additional drag coefficient caused by the retracted dive-recovery flaps was small and its variation with Mach number is shown in figure 11.

### CONCLUSIONS

High-speed tests of a 1/3-scale model of a single-engine pursuit airplane showed the following effects of Mach number on the longitudinal stability and on the effectiveness of the tail and the elevator:

1. An increase in the Mach number from 0.4 to 0.8 caused an increase of 160 percent in the static longitudinal stability. There was a corresponding decrease of 0.19 in the lift coefficient for balance with the elevator neutral.

2. Changes of tail and elevator effectiveness with Mach number were small but sufficient to cause the ratio of tail to elevator effectiveness to increase from 1.5 at 0.4 Mach number to 2.1 at 0.765 Mach number for small angles of attack.

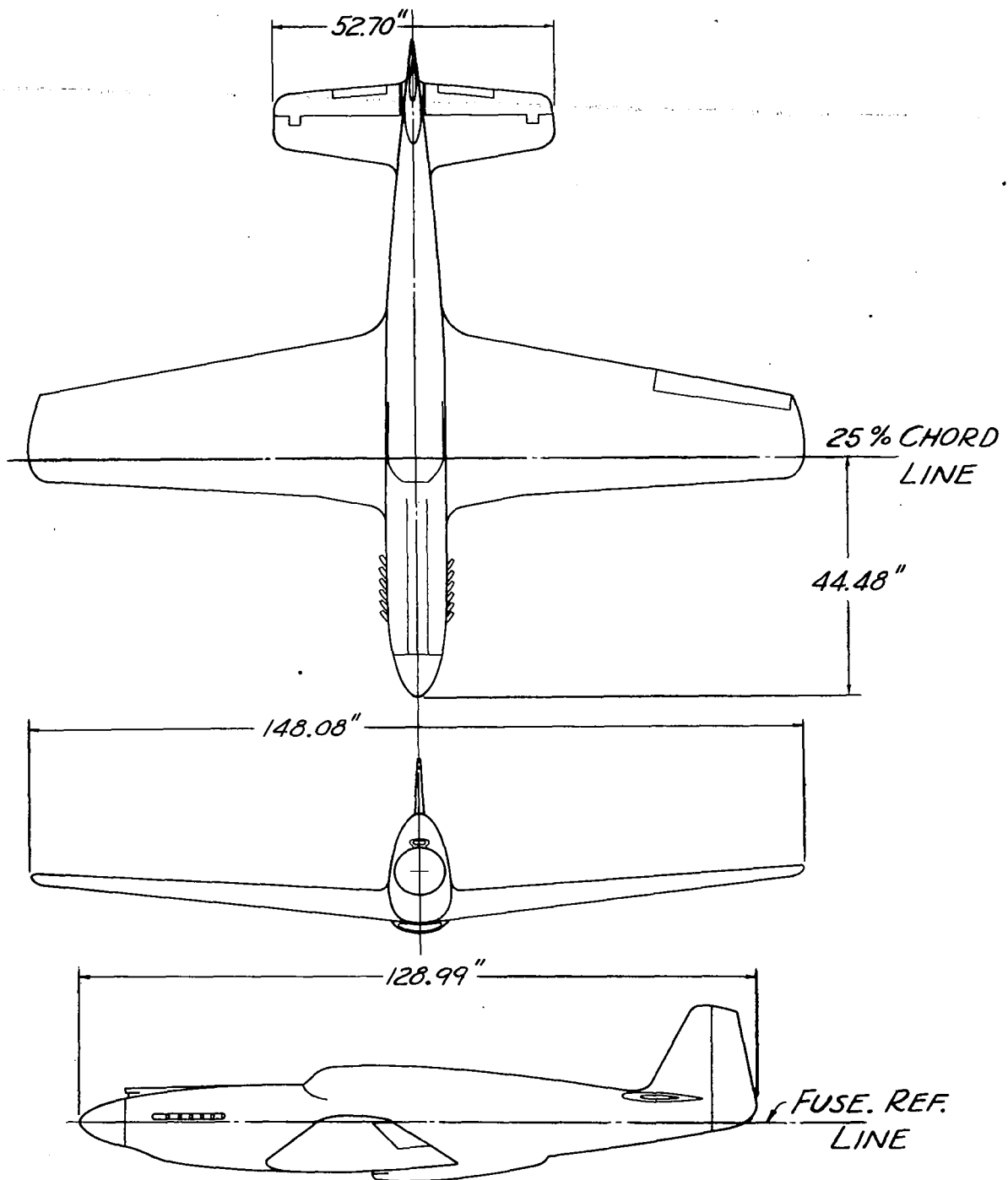
3. The small increments in drag and pitching-moment coefficients caused by the cooling-air deflector vane do not explain the effect this vane was reported to have on longitudinal oscillations of the airplane when diving.

Amos Aeronautical Laboratory,  
National Advisory Committee for Aeronautics,  
Moffett Field, Calif., May 3, 1945.

## REFERENCES

1. Hall, Charles F.: The Effect of Modifications to the Horizontal Tail Profile on the High-Speed Longitudinal Control of a Pursuit Airplane. NACA TN No. 1302, 1947.
2. Nissen, James M., Gadoborg, Burnett L., and Hamilton, William T.: Correlation of the Drag Characteristics of a P-51B Airplane Obtained From High-Speed Wind-Tunnel and Flight Tests. NACA ACR No. 4K02, 1945.
3. Silverstein, Abe, and White, James A.: Wind-Tunnel Interference With Particular Reference to Off-Center Positions of the Wing and to the Downwash at the Tail. NACA Rep. No. 547, 1935.

*but ref 3 does not  
apply to wind tunnel!*



NATIONAL ADVISORY  
COMMITTEE FOR AERONAUTICS

FIGURE 1.- THREE-VIEW DRAWING OF THE  
 $\frac{1}{3}$ -SCALE MODEL.

MR No. A5E03

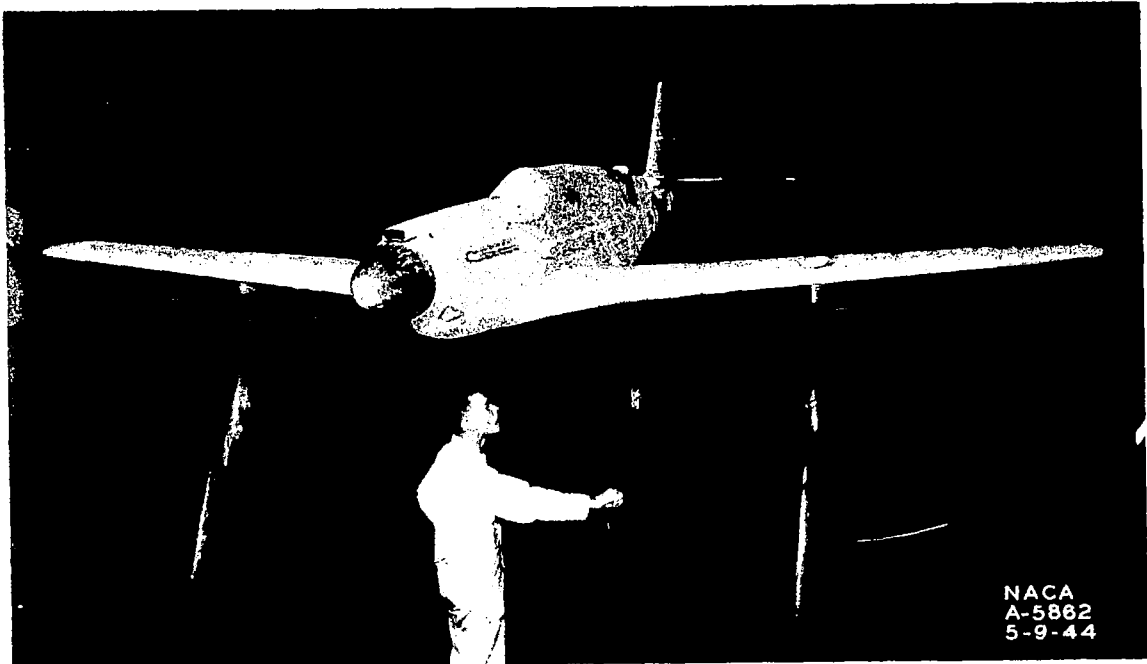


Figure 2.- The 1/3-scale model in the 16-foot wind tunnel (5-percent-thick front struts spaced 80 inches, 7-percent-thick rear strut).

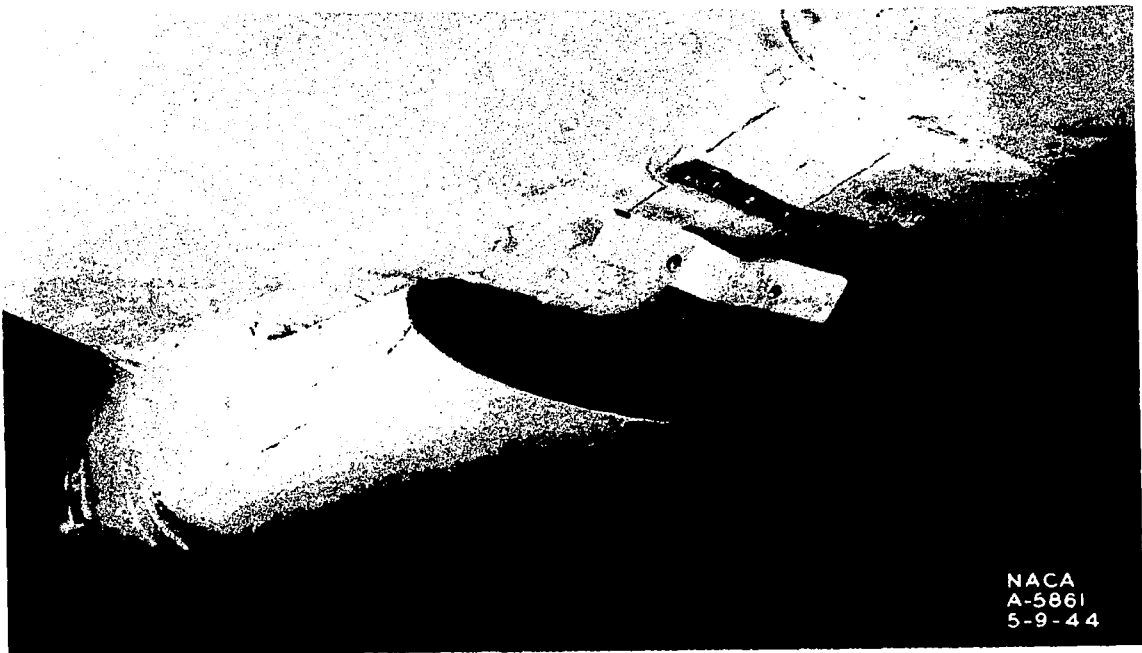


Figure 3.- Deflector vane in front of the cooling duct on the model.

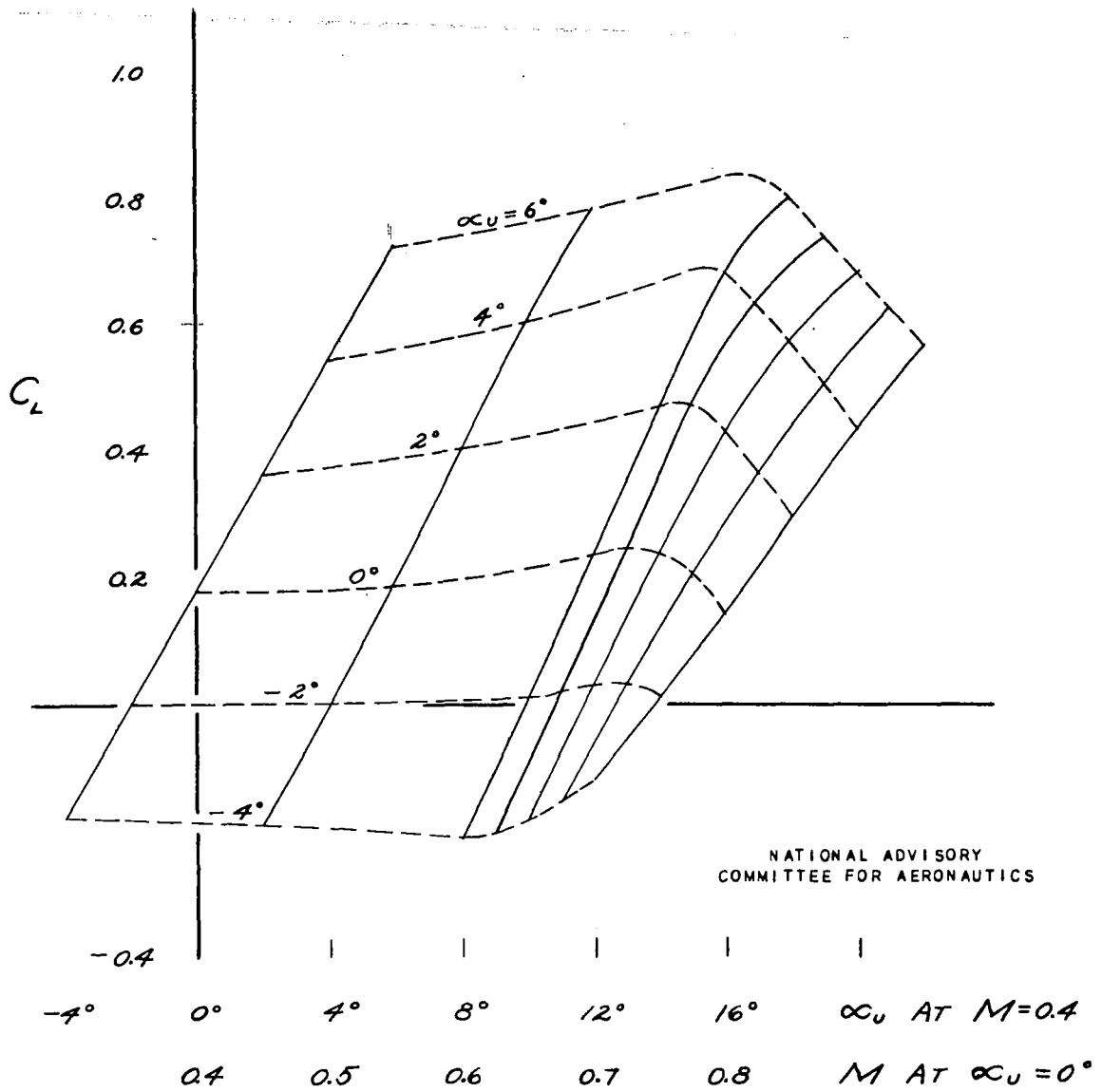


FIGURE 4.- THE LIFT COEFFICIENT CARPET FOR THE  $\frac{1}{3}$ -SCALE MODEL WITHOUT A TAIL.

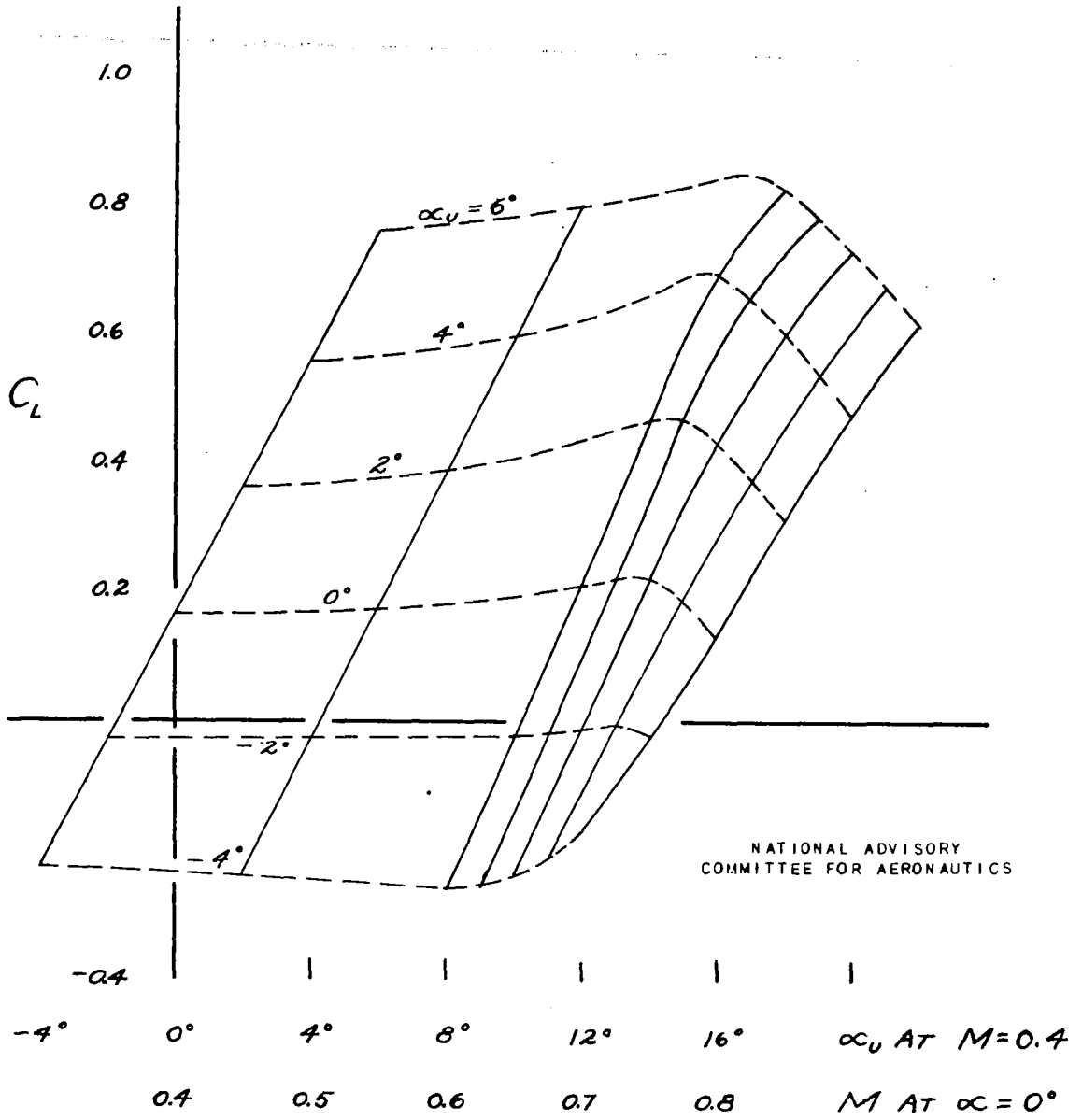


FIGURE 5.- THE LIFT COEFFICIENT CARPET FOR THE  $\frac{1}{3}$ -SCALE MODEL.  $i_t, 2^\circ$ ;  $\delta_e, 0^\circ$ .

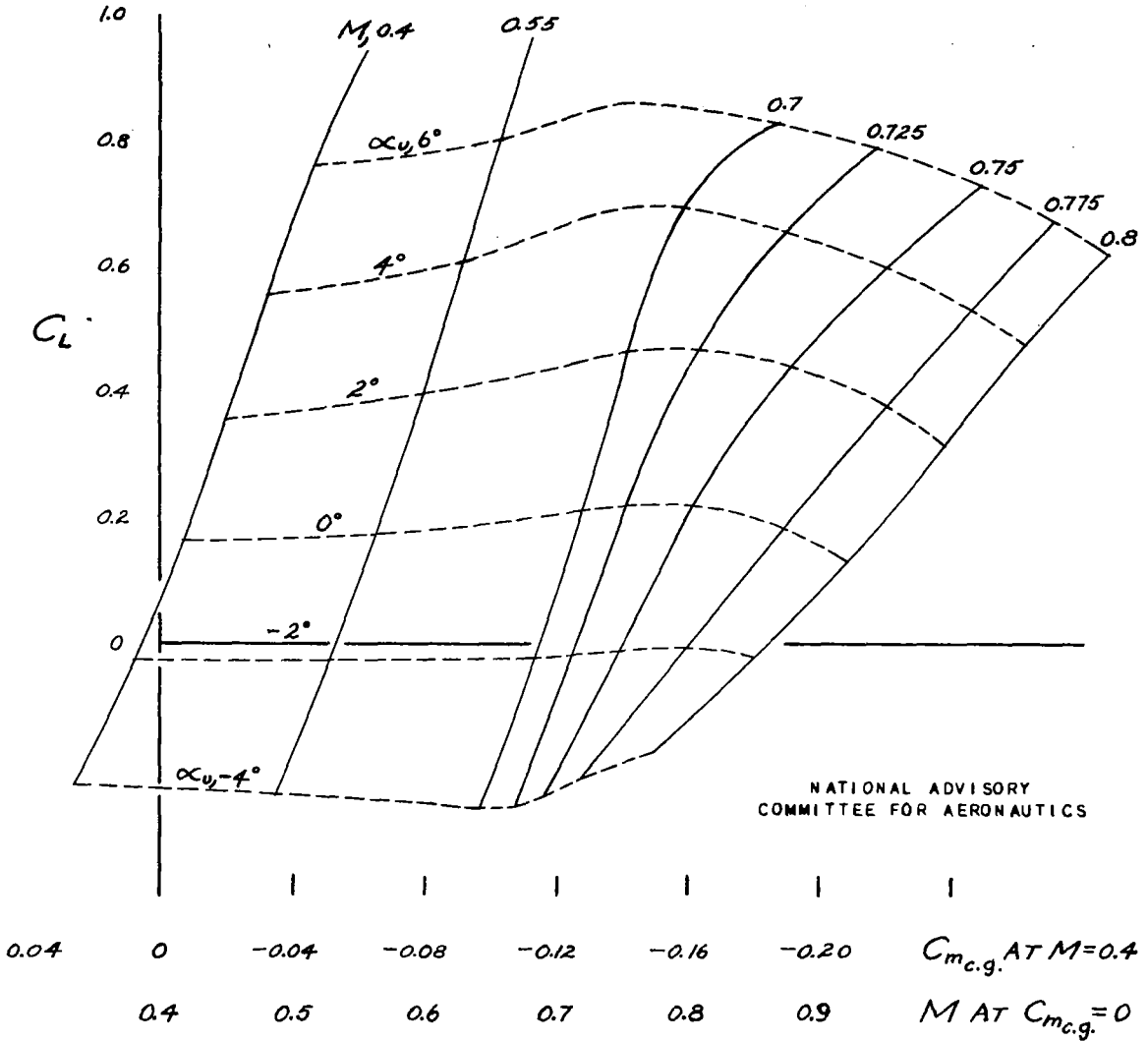
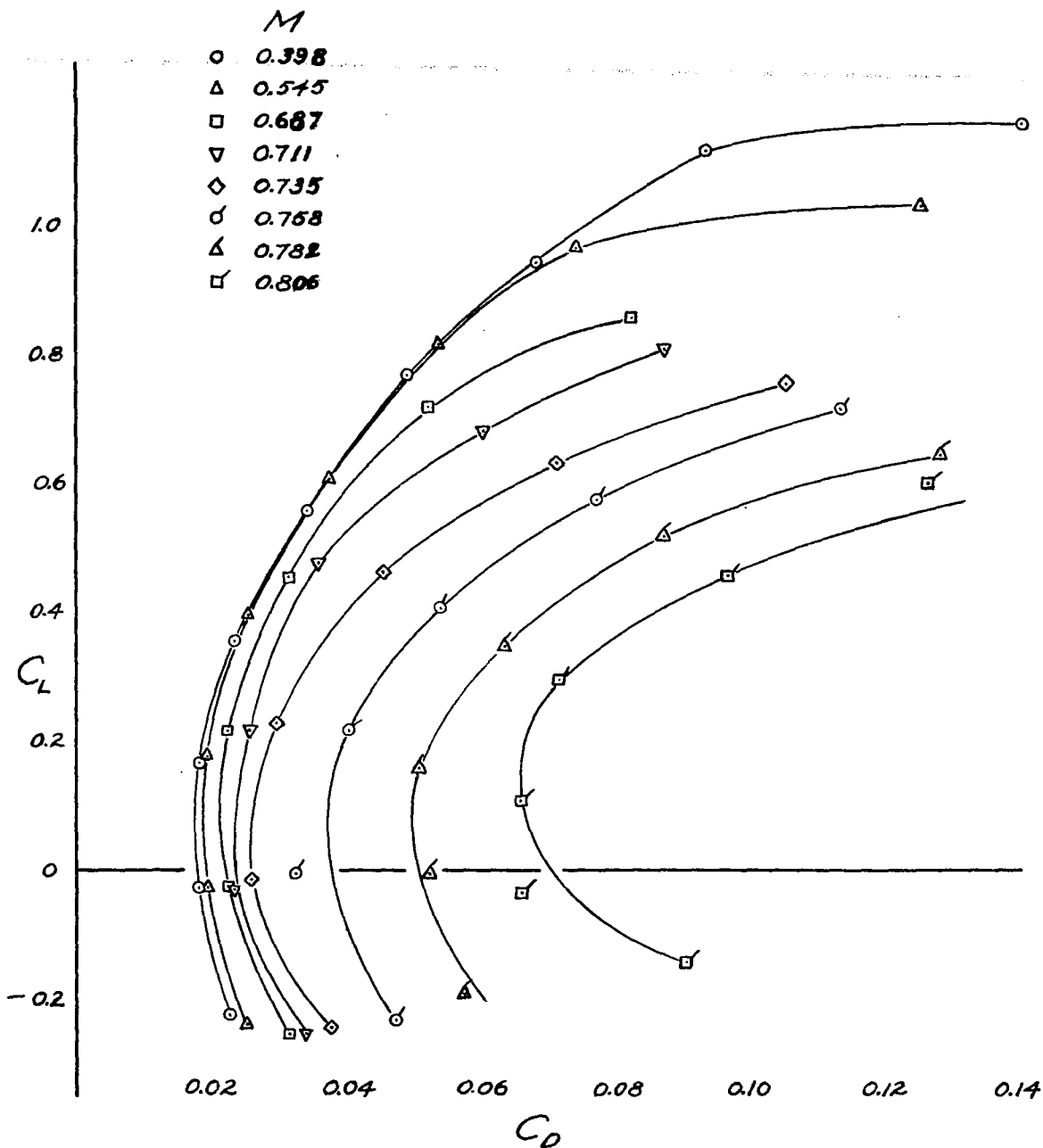


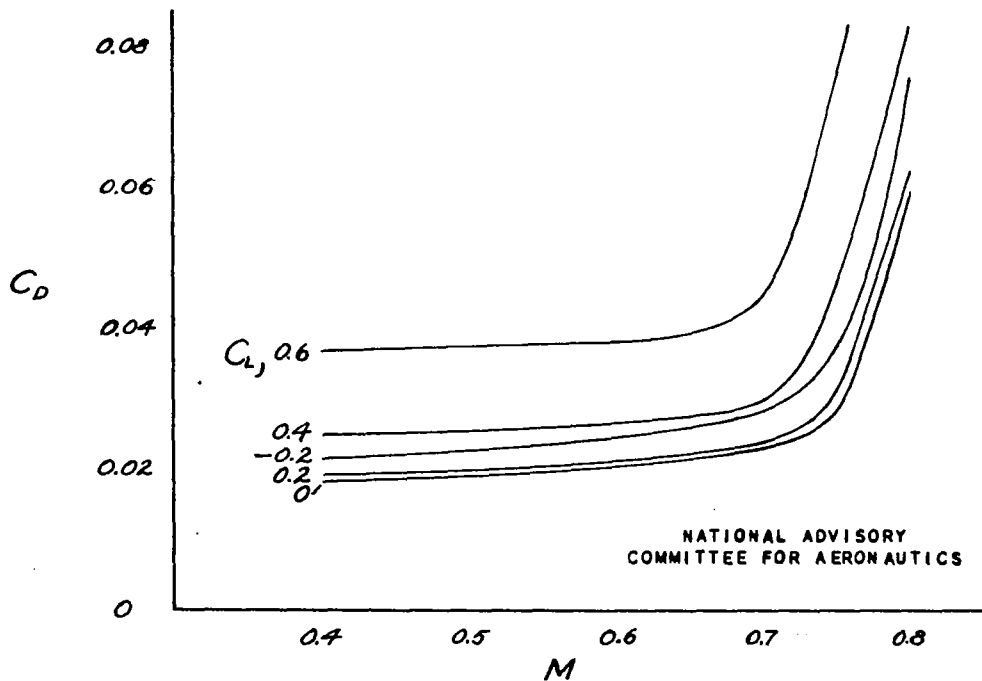
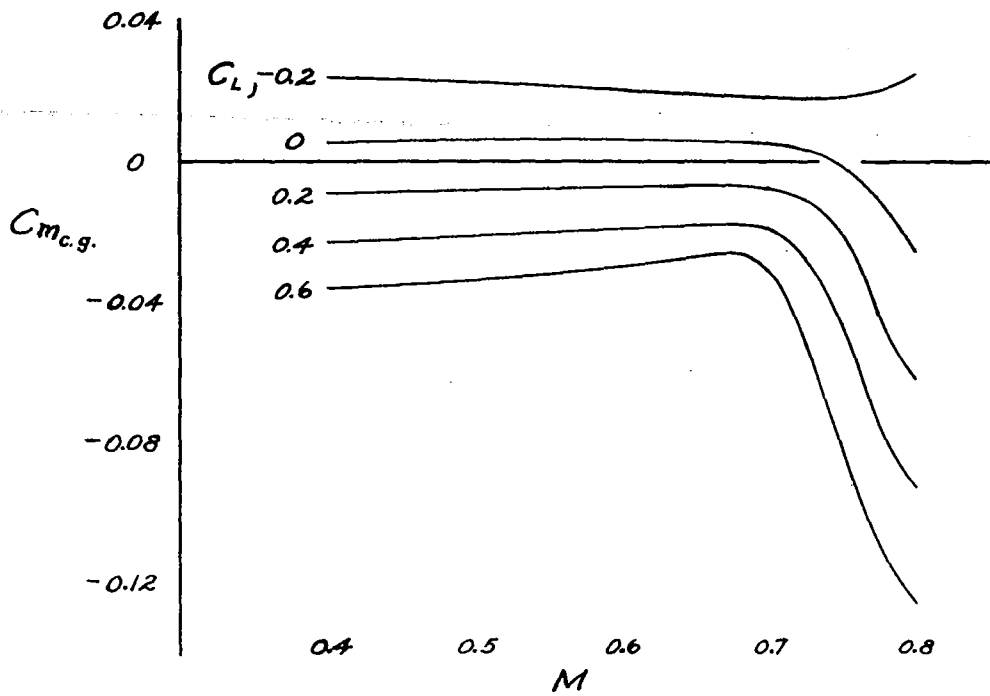
FIGURE 6.- THE PITCHING-MOMENT-COEFFICIENT CARPET FOR THE  $\frac{1}{3}$ -SCALE MODEL.  $i_t, 2^\circ$ ;  $\delta_e, 0^\circ$ .



NATIONAL ADVISORY  
COMMITTEE FOR AERONAUTICS

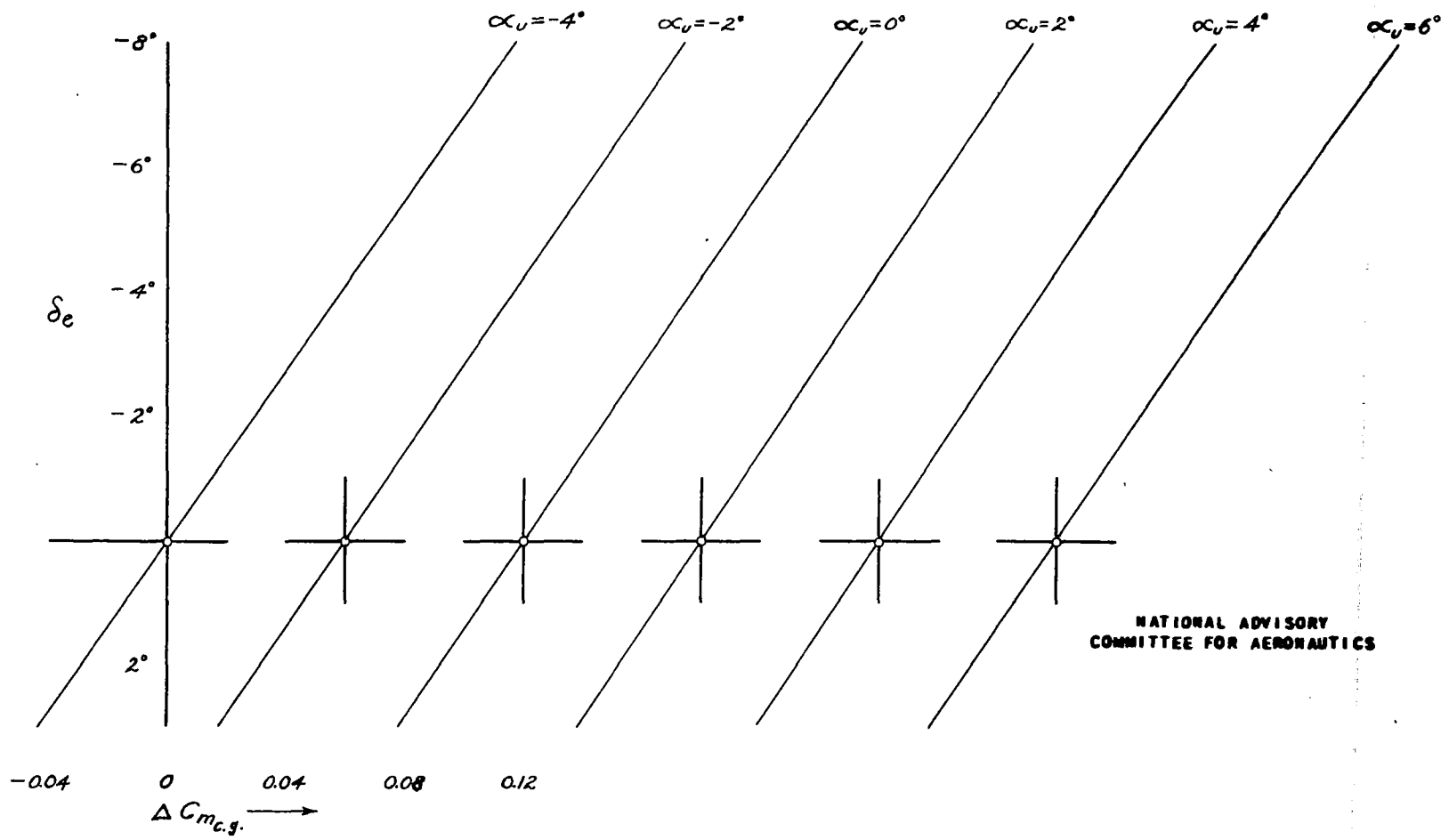
FIGURE 7.- THE VARIATION OF DRAG COEFFICIENT WITH LIFT COEFFICIENT FOR SEVERAL VALUES OF MACH NUMBER.





NATIONAL ADVISORY  
COMMITTEE FOR AERONAUTICS

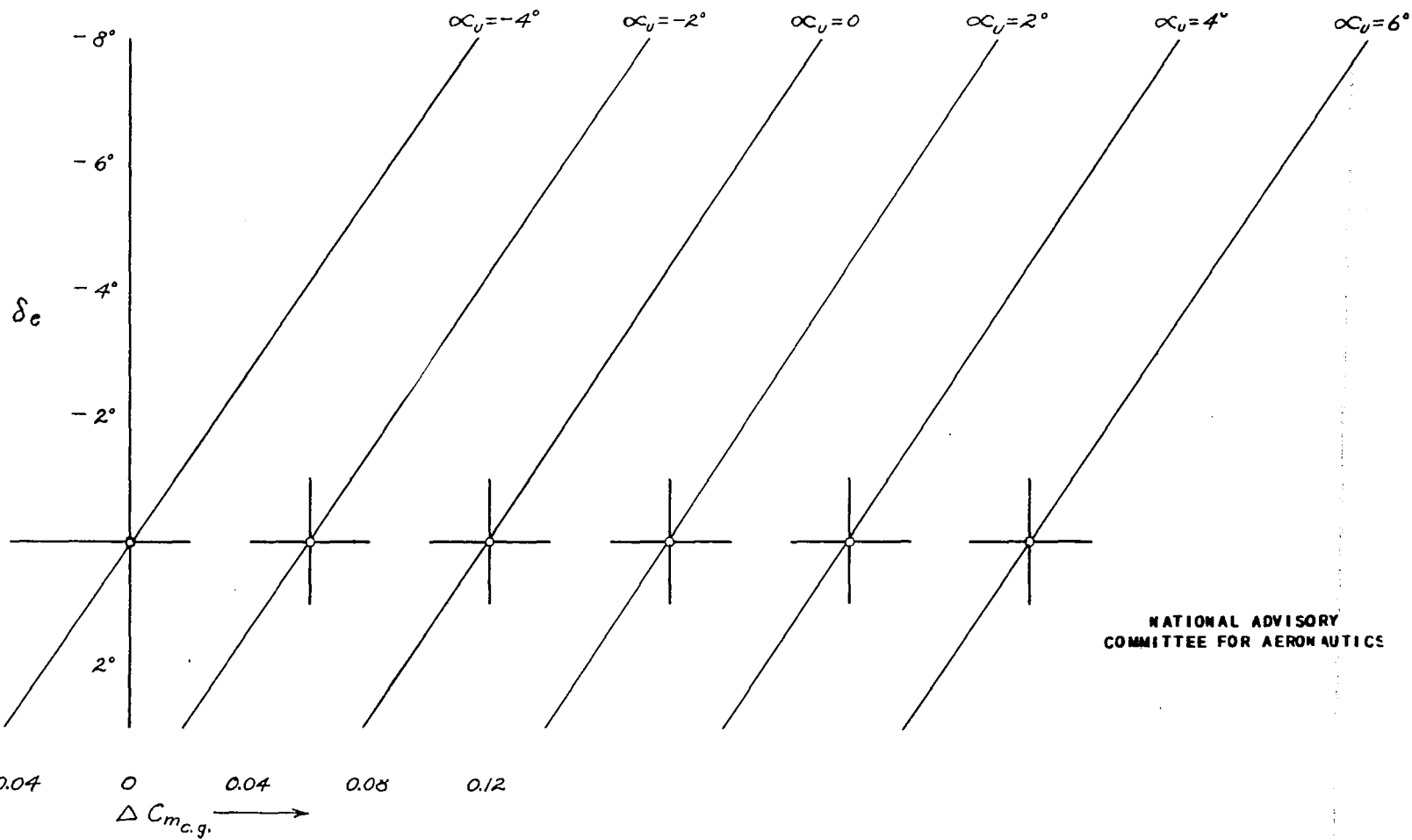
FIGURE 8.- THE VARIATION OF PITCHING-MOMENT AND DRAG COEFFICIENTS WITH MACH NUMBER AT SEVERAL VALUES OF LIFT COEFFICIENT.



NATIONAL ADVISORY  
COMMITTEE FOR AERONAUTICS

(a)  $M=0.4$

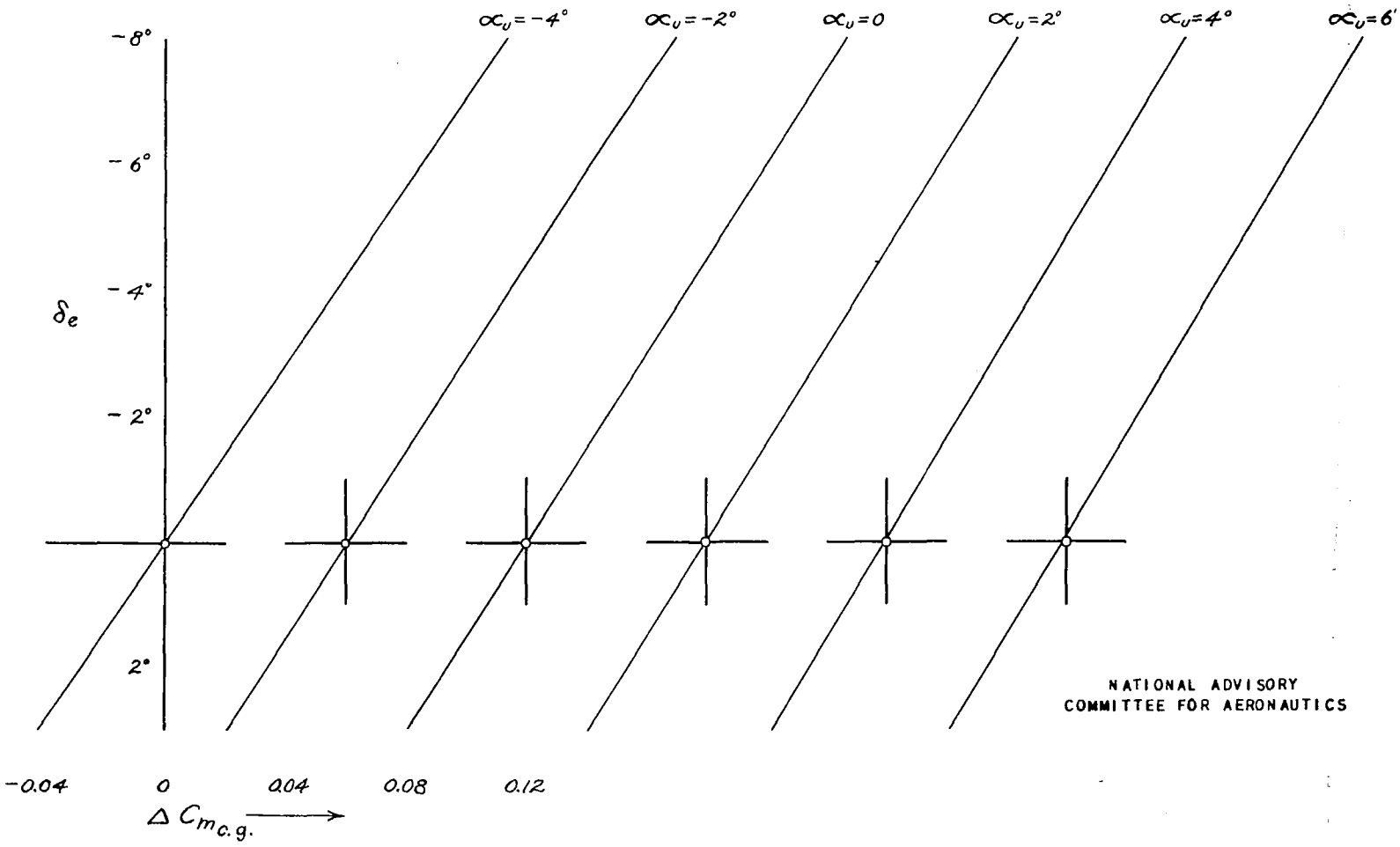
FIGURE 9.- THE INCREMENT IN PITCHING-MOMENT COEFFICIENT DUE TO ELEVATOR DEFLECTION FOR SEVERAL ANGLES OF ATTACK.



NATIONAL ADVISORY  
COMMITTEE FOR AERONAUTICS

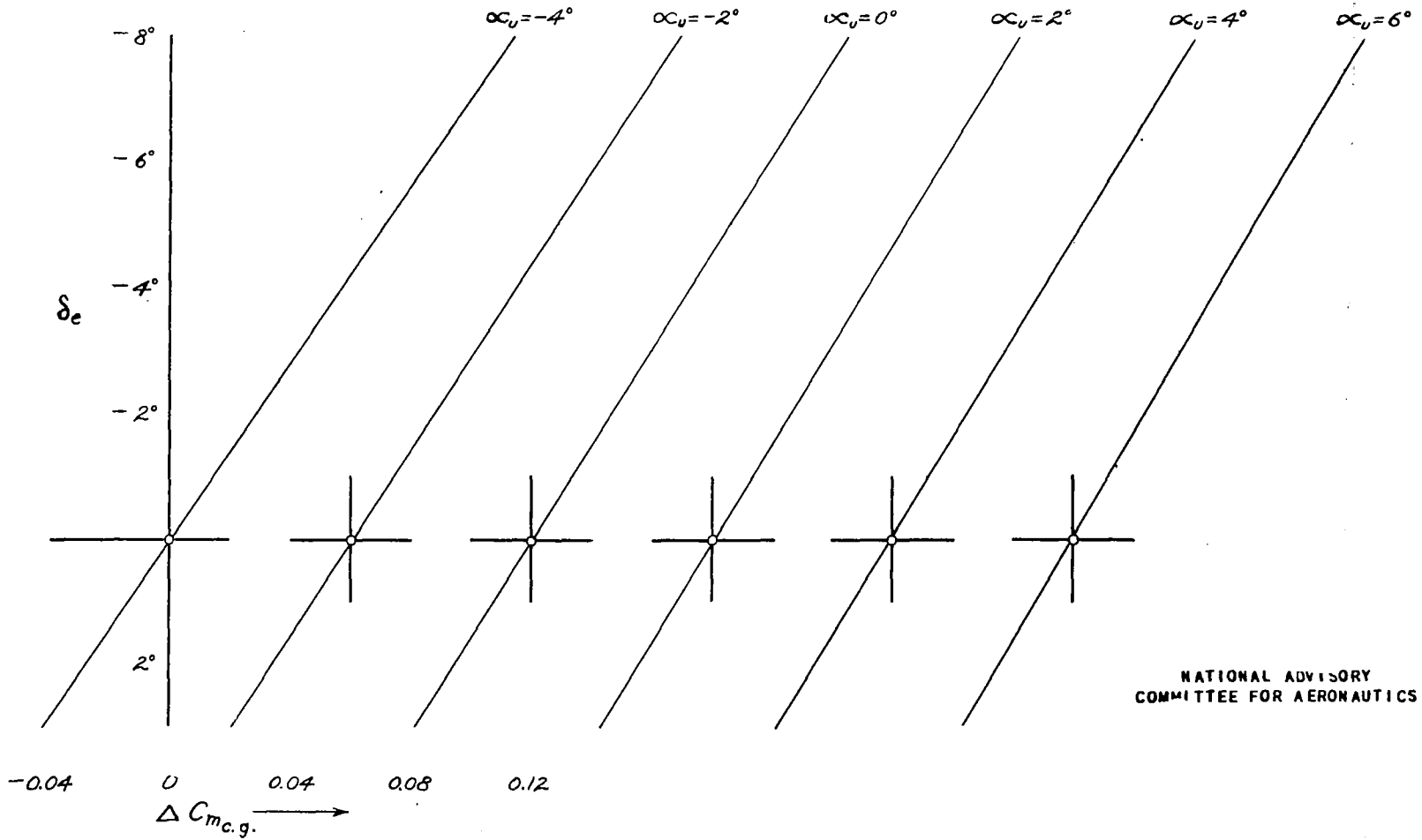
(b)  $M = 0.55$ .

FIGURE 9.- CONTINUED.



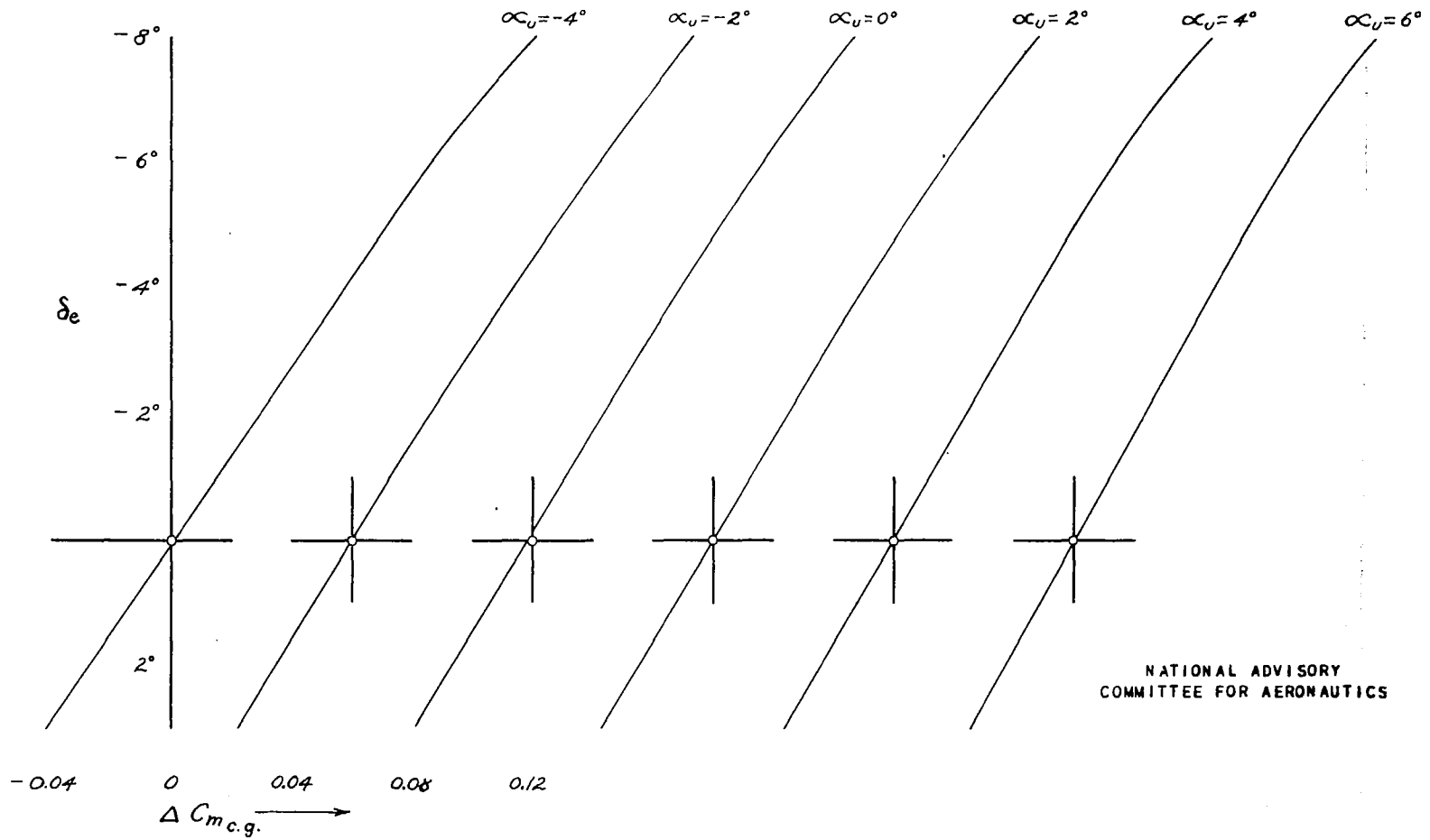
NATIONAL ADVISORY  
COMMITTEE FOR AERONAUTICS

(C)  $M=0.7$   
FIGURE 9.- CONTINUED.



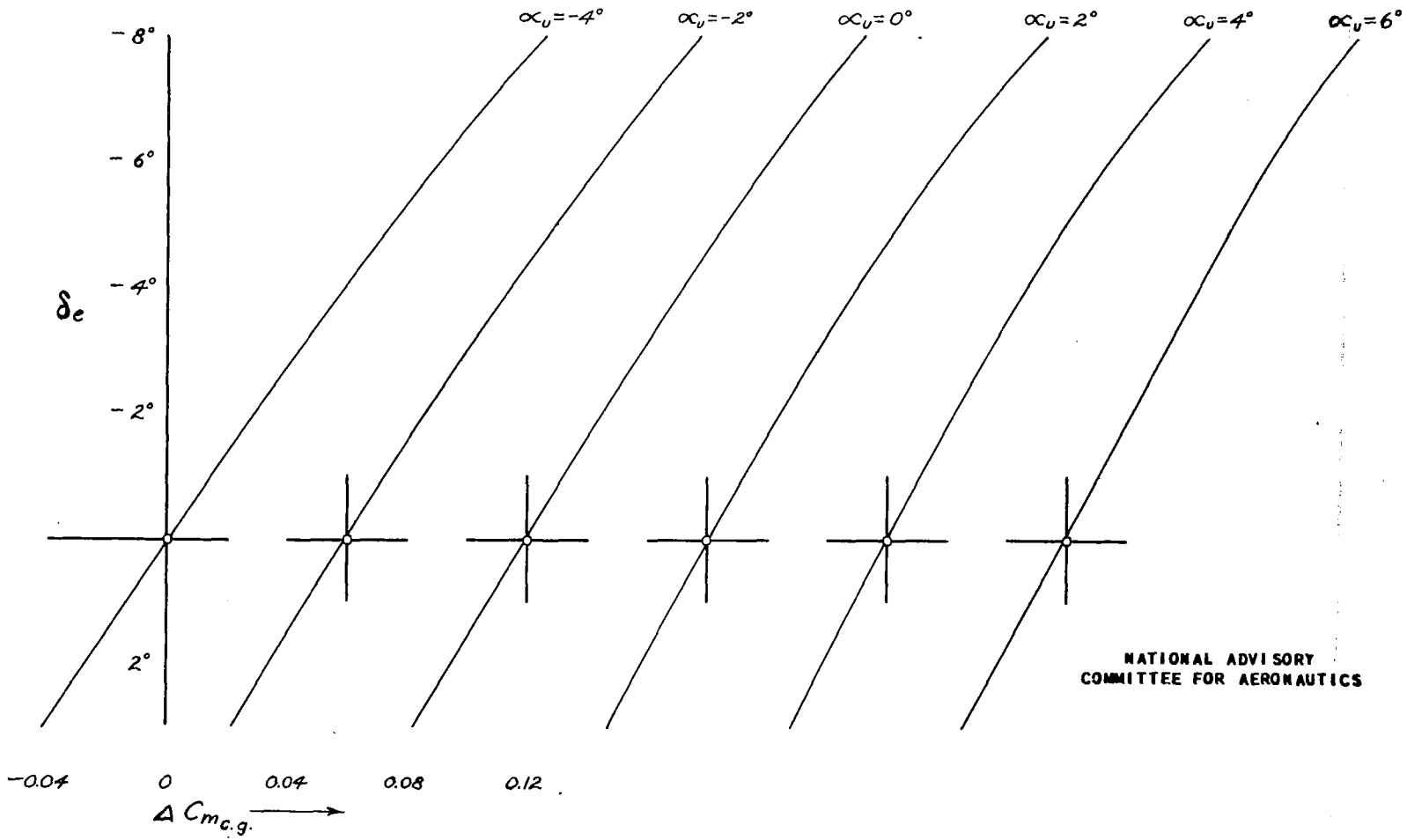
NATIONAL ADVISORY  
COMMITTEE FOR AERONAUTICS

(d)  $M=0.725$   
FIGURE 9.— CONTINUED.



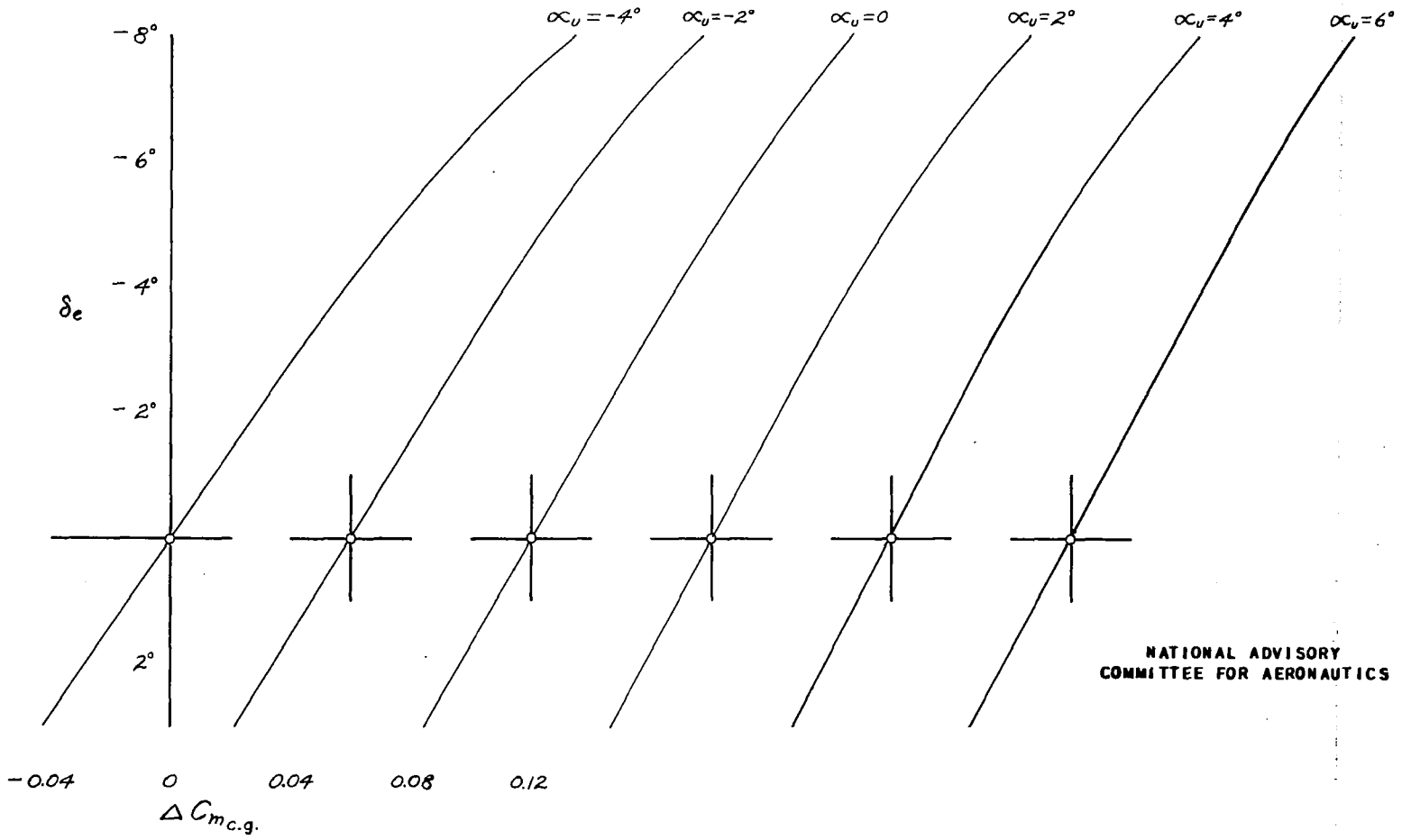
NATIONAL ADVISORY  
COMMITTEE FOR AERONAUTICS

(e)  $M = 0.75$   
FIGURE 9.- CONTINUED.



NATIONAL ADVISORY  
COMMITTEE FOR AERONAUTICS

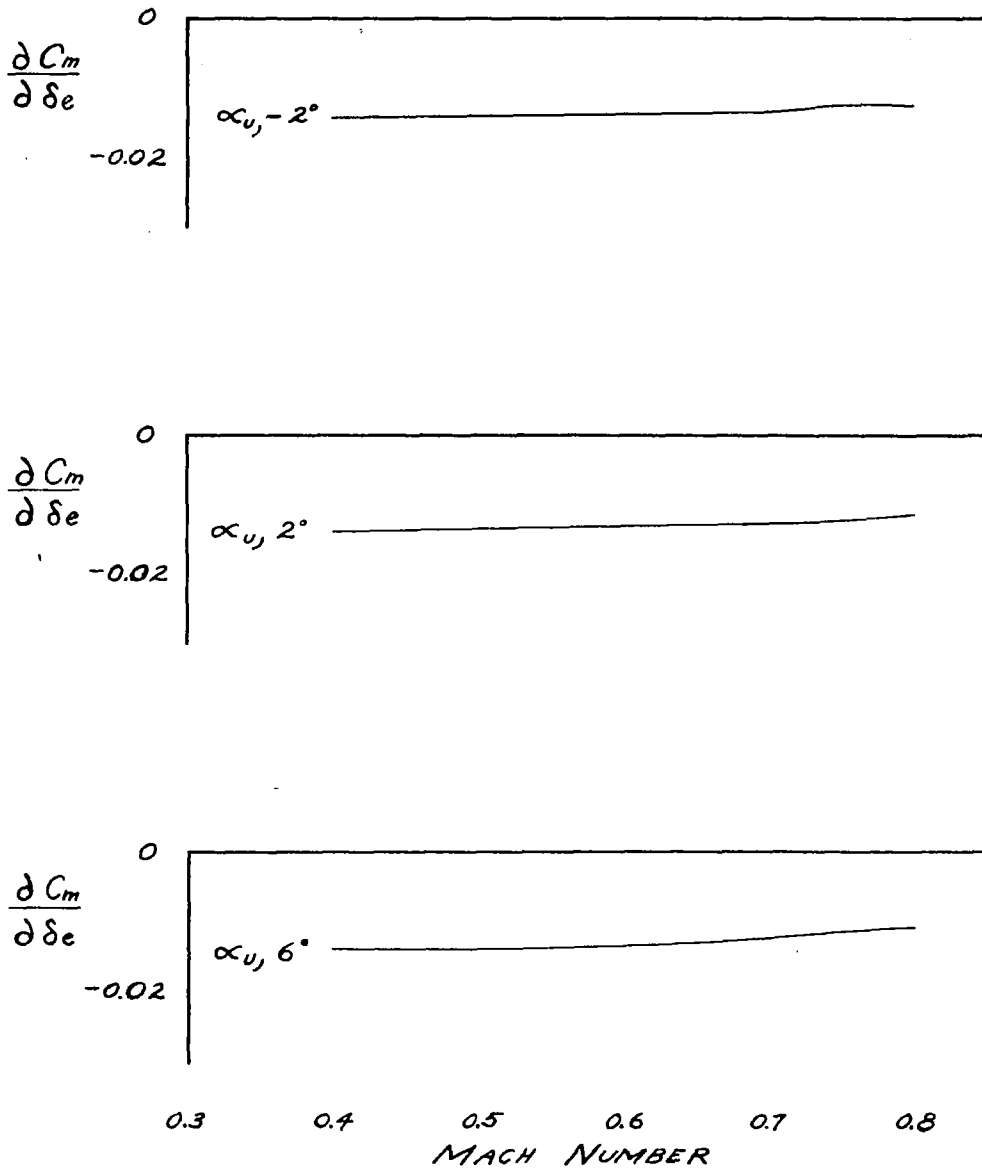
(f)  $M=0.775$   
FIGURE 9.- CONTINUED.



NATIONAL ADVISORY  
COMMITTEE FOR AERONAUTICS

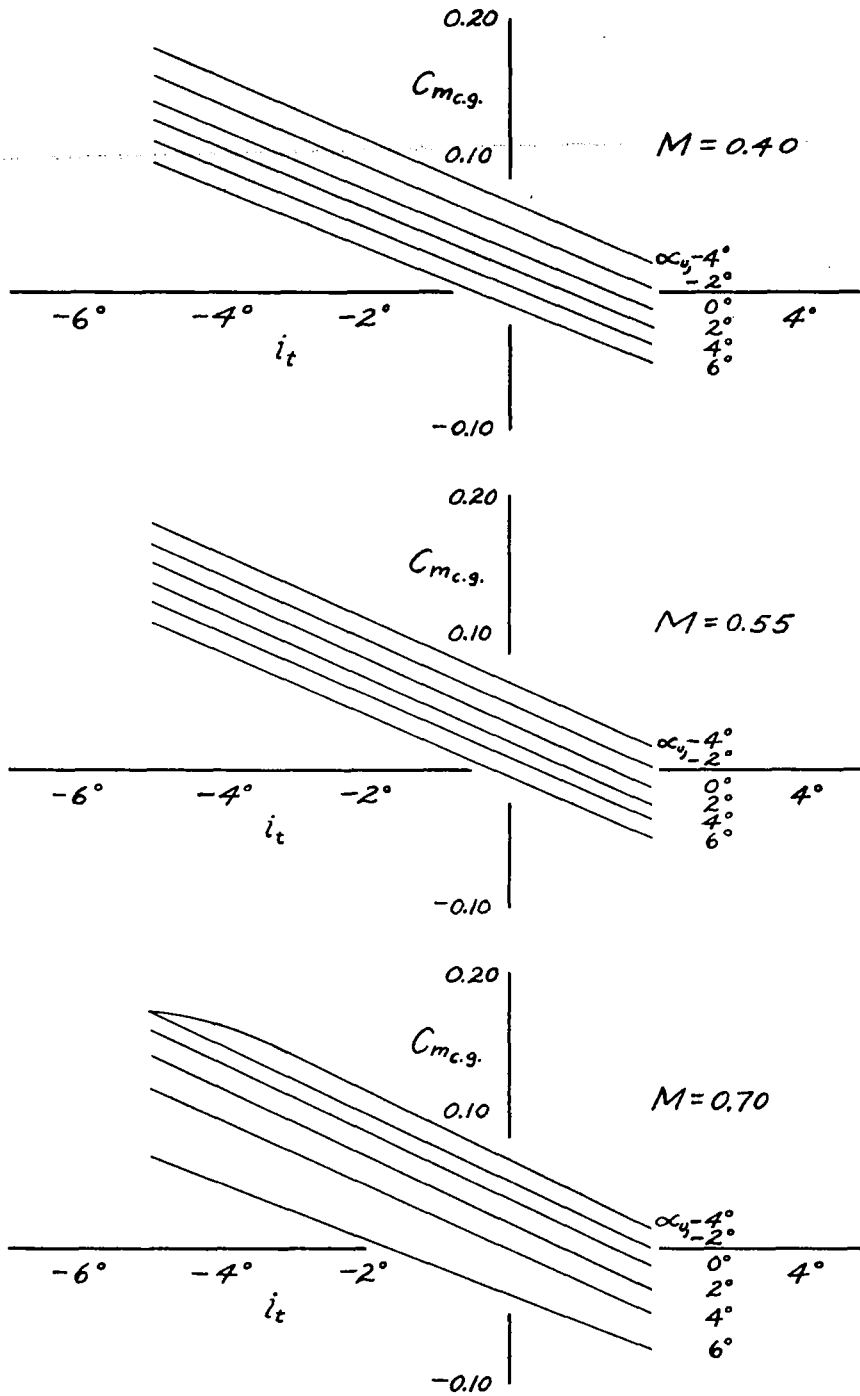
(9)  $M=0.8$   
FIGURE 9.- CONCLUDED.





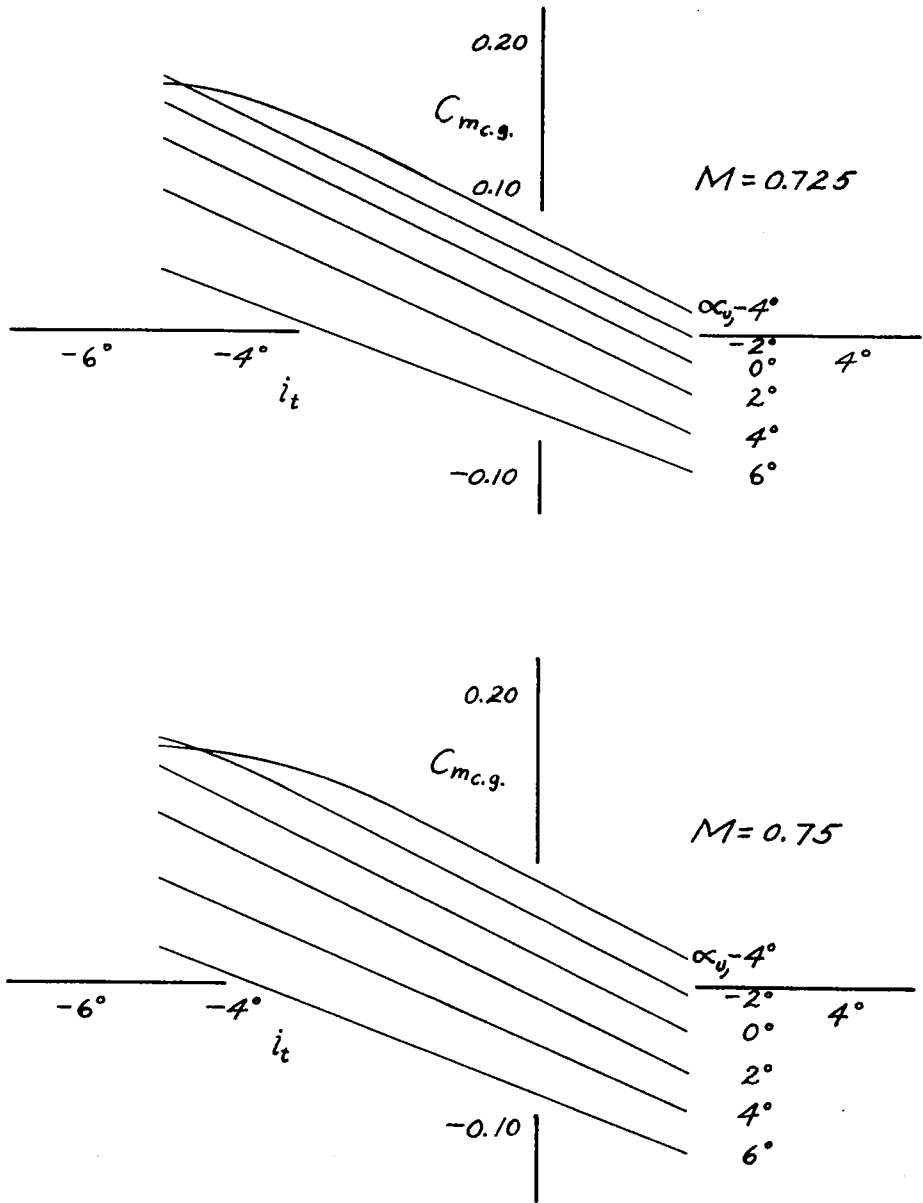
NATIONAL ADVISORY  
COMMITTEE FOR AERONAUTICS

FIGURE 10.— THE VARIATION OF ELEVATOR EFFECTIVENESS WITH MACH NUMBER FOR THREE ANGLES OF ATTACK.  $i_t, 2^\circ$



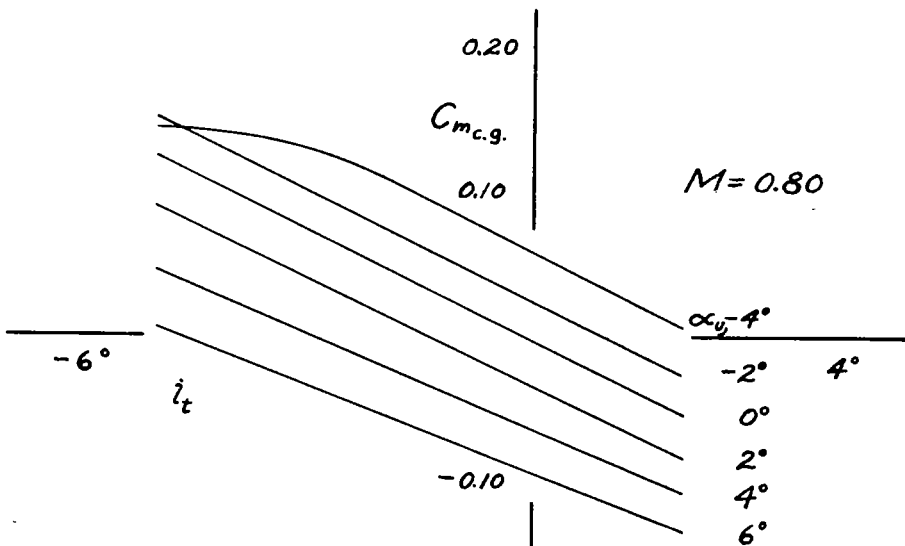
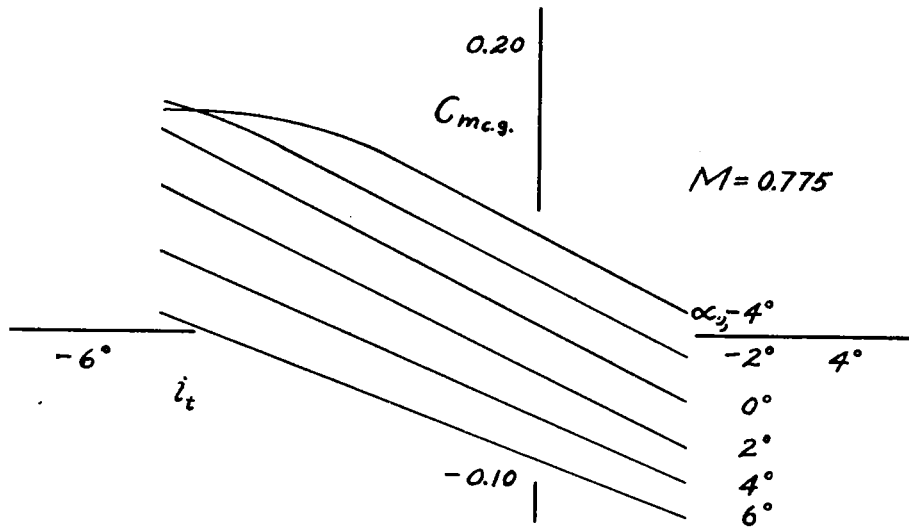
NATIONAL ADVISORY  
COMMITTEE FOR AERONAUTICS

(a)  $M=0.4, 0.55, \text{ and } 0.7.$   
 FIGURE 11.- THE VARIATION OF PITCHING-MOMENT  
 COEFFICIENT WITH TAIL INCIDENCE FOR  
 SEVERAL ANGLES OF ATTACK.  $\delta_e, 0^\circ.$



NATIONAL ADVISORY  
COMMITTEE FOR AERONAUTICS

(b)  $M = 0.725$  AND  $0.75$   
FIGURE 11.- CONTINUED.



NATIONAL ADVISORY  
COMMITTEE FOR AERONAUTICS

(C)  $M = 0.775$  AND  $0.8$   
FIGURE 11.- CONCLUDED.

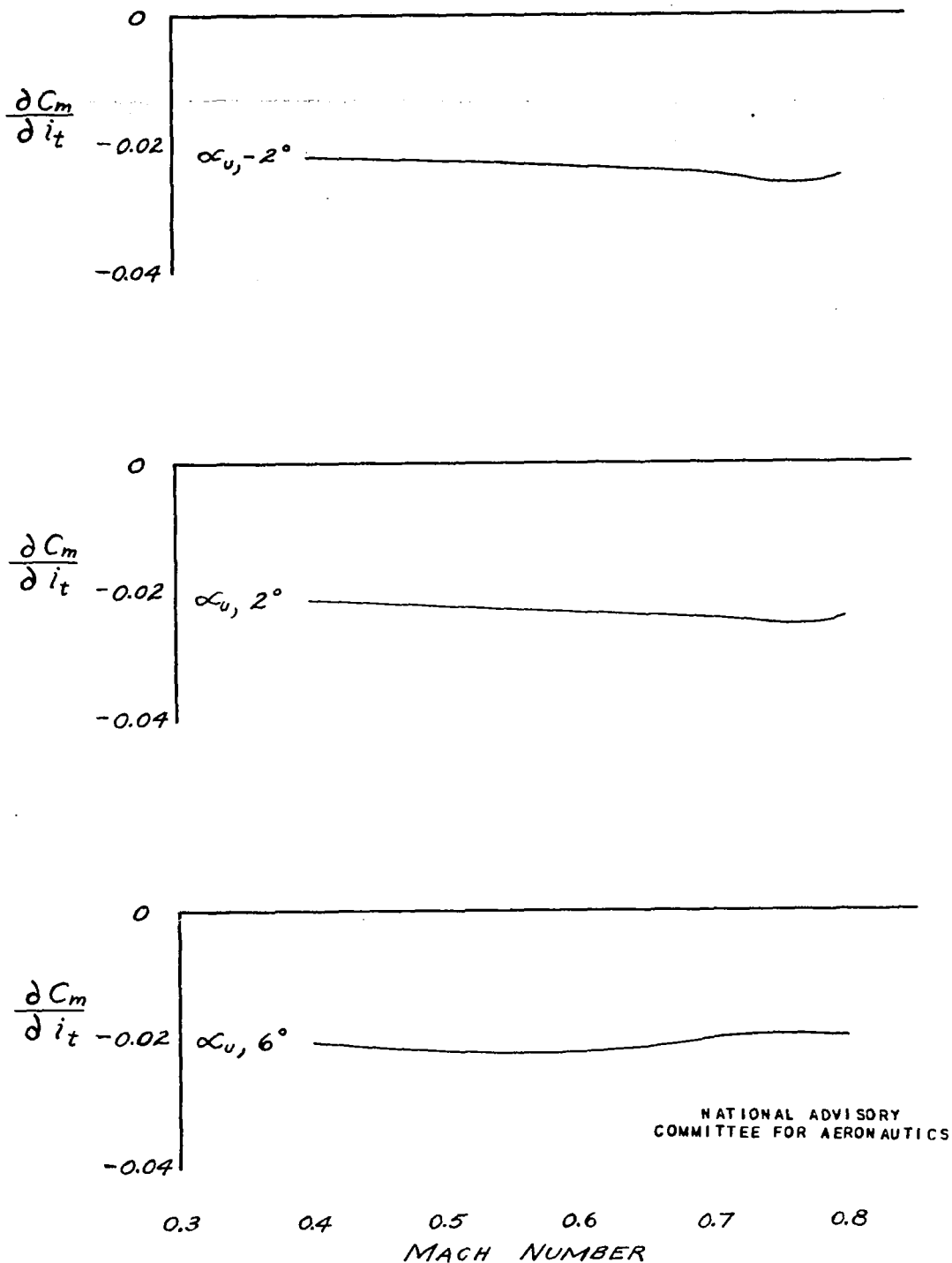


FIGURE 12.- THE VARIATION OF TAIL EFFECTIVENESS WITH MACH NUMBER FOR THREE ANGLES OF ATTACK.  $\delta_e, 0^\circ$ .

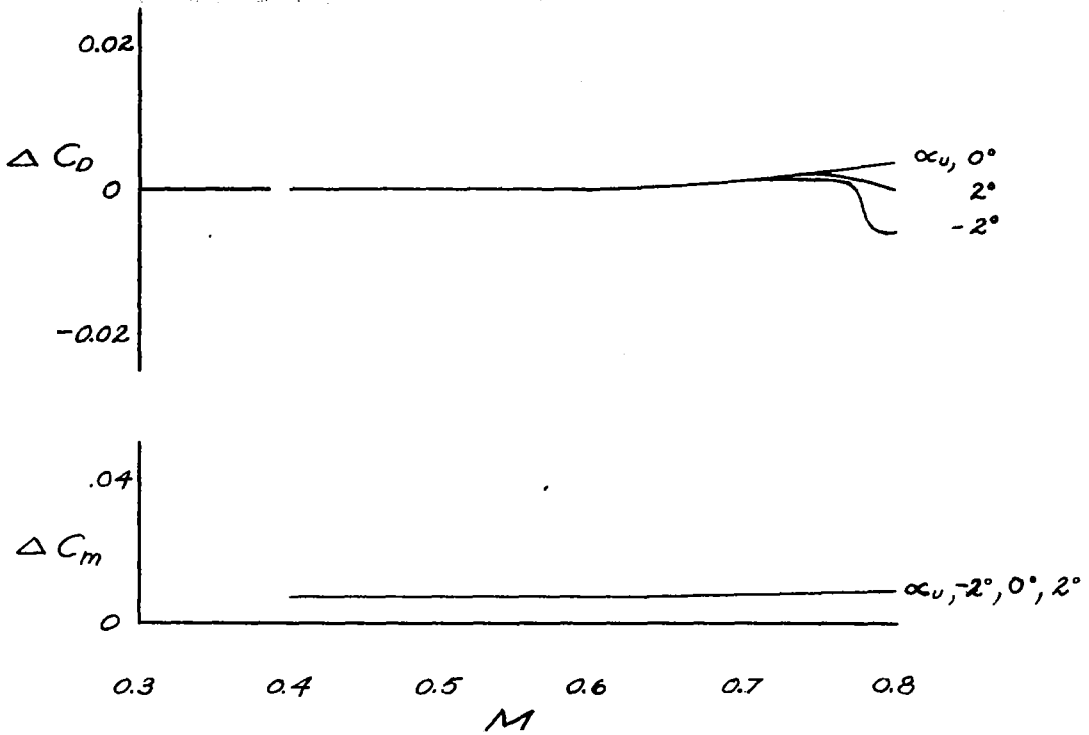
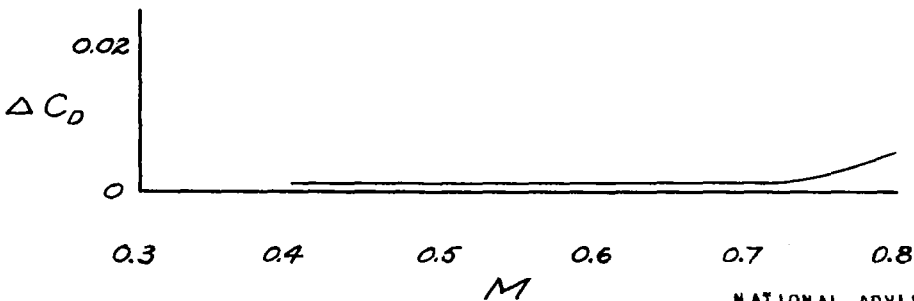


FIGURE 13.- ADDITIONAL DRAG AND PITCHING-MOMENT COEFFICIENT FROM THE DEFLECTOR VANE.



NATIONAL ADVISORY  
COMMITTEE FOR AERONAUTICS

FIGURE 14.- ADDITIONAL DRAG COEFFICIENT FROM THE RETRACTED DIVE-RECOVERY FLAPS.

NASA Technical Library



3 1176 01403 1604